Energy Conversion and Management 84 (2014) 97–107

Contents lists available at ScienceDirect

Energy Conversion and Management

journal homepage: www.elsevier.com/locate/enconman

Comparisons of system benefits and thermo-economics for exhaust energy recovery applied on a heavy-duty diesel engine and a light-duty vehicle gasoline engine

Tianyou Wang [a,*], Yajun Zhang [a], Jie Zhang [a], Zhijun Peng [b], Gequn Shu [a]

[a] State Key Laboratory of Engines, Tianjin University, China
[b] Science & Technology Research Institute, University of Hertfordshire, UK

ARTICLE INFO

Article history:
Received 3 February 2014
Accepted 4 April 2014
Available online 4 May 2014

Keywords:
Exhaust energy recovery
Rankine cycle
Diesel engine
Gasoline engine
Working fluid

ABSTRACT

Exhaust energy recovery system (EERS) based on Rankine cycle (RC) in internal combustion engines have been studied mainly on heavy-duty diesel engines (D) and light-duty vehicle gasoline engines (G), however, little information available on systematical comparisons and evaluations between the two applications, which is a particularly necessary summary for clarifying the differences. In this paper, the two particular systems are compared quantitatively using water, R141b, R123 and R245fa as working fluids. The influences of evaporating pressure, engine type and load on the system performances are analyzed with multi-objectives, including the thermal efficiency improvement, the reduced CO_2 emission, the total heat transfer area per net power output (*APP*), the electricity production cost (*EPC*) and the payback period (*PBP*). The results reveal that higher pressure and engine load would be attractive for better performances. R141b shows the best performances in system benefits for the D-EERS, while water exhibits the largest contributions in the G-EERS. Besides, water performs the best thermo-economics, and R245fa serves as the most uneconomical fluid. The D-EERS presents superior to the G-EERS in the economic applicability as well as much more CO_2 emission reductions, although with slightly lower thermal efficiency improvement, and only the D-EERS with water under the full load meets the economic demand. Therefore the EERS based on RC serve more applicable on the heavy-duty diesel engine, while it might be feasible for the light-duty vehicle gasoline engine as the state-of-the art technologies are developed in the future.

1. Introduction

Greenhouse effect and depleted petroleum supplies have urged the harsh demands on the fuel economy improvements of internal combustion engine (ICE). Therefore, waste heat recovery (WHR) technology based on Rankine cycle (RC) is getting revived and paid much attention in recent years. The ICE equipped with a RC system could have a considerable improvement by up to 10–15% in fuel consumption [1].

Reviewing the literatures in the past decades, most of the studies were aimed at the application to heavy-duty diesel engine trucks, ships, and generators, etc. due to the stable operations and high quantity of waste heat. Early in 1980s, Patel and Doyle [2] made a conceptual design study of compounding a long haul diesel truck engine with an organic RC system. DiNanno et al. [3,4] also tested an organic RC system compounded on a class 8 diesel engine with 288 brake horsepower. Recent examples using the RC for WHR can be found from the experimental researches conducted by Teng et al. [5–7], which demonstrated up to 20% of waste heat from the heavy-duty diesel engine may be recovered, making the efficiency for the hybrid energy system be over 50%. Hountalas et al. [8,9] provided theoretical simulations and experimental design of RC applied on a heavy-duty diesel engine used in long haul trucks to estimate the potential efficiency gain from its application and the attempts to resolve technical challenges such as system packaging and excess coolant heat rejection. Macián et al. [10] presented a methodology for the optimization of a bottoming cycle for recovering various waste heat sources from a heavy duty diesel engine. Other researches include the work of Shu et al. [11–13], who compared several dual-loop organic RC systems to explore the best combined system and working fluids for the maximum utilization of WHR from diesel engine.

* Corresponding author. Address: No. 92, Weijin Road, Nankai District, Tianjin, China. Tel.: +86 (0)22 2740 3434; fax: +86 (0)22 2740 6890.
E-mail address: wangtianyou@tju.edu.cn (T. Wang).

http://dx.doi.org/10.1016/j.enconman.2014.04.022
0196-8904/

Nomenclature

a	specific amount (kg/(kW h))
A	overall heat transfer area (m^2)
APP	total heat transfer area per net power output (m^2/(kW))
C_{bm}	component cost ($/year)
Cc	system capital cost ($/year)
$CEPCI$	Chemical Engineering Plant Cost Index
Com	operation and management cost ($/year)
c_p	specific heat of exhaust gas (J/(kgK))
C_{pri}	average price of diesel or gasoline (¥/t)
CRF	capital recovery cost
C_t	temperature difference correction factor
d	diameter (m)
D	heavy-duty diesel engine
EERS	exhaust energy recovery system
EI	thermal efficiency improvement
EPC	electricity production cost ($/(kW h))
f	resistance coefficient
G	light-duty vehicle gasoline engine
h	specific enthalpy (kJ/kg)
i	interest rate
ICE	internal combustion engine
LMTD	logarithmic mean temperature difference
LT	system operation lifetime (year)
m	mass flow rate (kg/s)
M	amount (kg/year)
Nu	Nusselt number
p	pressure (MPa)
Pr	Prandtl number
PBP	payback period (year)
PPTD	pinch point temperature difference
Q	heat transfer rate (kW)
R	net return per year ($/year)
RC	Rankine cycle
Re	Reynolds number
t	overall operating time per year (h)
T	temperature (°C)
U	overall heat transfer coefficient (W/(m^2 K))
W	work (kW)
WHR	waste heat recovery
α	heat transfer coefficient (W/(m^2 K))
ε	correction factor
η	efficiency
ρ	density (kg/m^3)
λ	thermal conductivity coefficient (W/(mK))

Subscripts

c	condenser
cw	cooling water
e	evaporator
eng	engine
exh	exhaust gases
i	inner
l	liquid state
o	outer
p	pump
t	turbine
v	vapor state
w	working fluid
1–7	states points in the cycle
0	atmosphere

Alternatively, much attention has also been paid on gasoline engines based on the considerations of low thermal efficiency and high exhaust gases temperature for the kind of engines. Stem from 1990s, Oomori and Ogino [14] combined the evaporative engine cooling system and Rankine bottoming system in search for the application possibility of Rankine bottoming system to passenger cars. In this century, Chammas and Clodic [15] presented the advantages of a Rankine system on a 1.4 L spark ignition engine for a typical passenger car, with potential for improving the net fuel consumption by up to 32%. Ringler et al. [16,17] employed a dual RC system for gasoline passenger car application and have recently developed a dynamic model of the evaporator for the WHR system. Arias et al. [18] and Endo et al. [19] proposed novel WHR systems to achieve the maximum potentials on gasoline automotive vehicle. Analysis based on experiments of a light duty gasoline engine by Wang et al. [20] predicted that the maximum exhaust energy recovery system (EERS) efficiency can be up to 14% under high engine power condition and 3–8% under general vehicle operating conditions. Wang et al. [21] analyzed the potential of a dual loop organic RC within the gasoline engine's entire operating region, and found that the relative output power improves by from 14% to 16% in the peak effective thermal efficiency region to 50% in the small load region, and the absolute effective thermal efficiency increases by 3–6% throughout the engine's operating region. Peng et al. [22] examined integrated EERS for light duty gasoline vehicle and hybrid electrical vehicle in the improvement on the total power-train efficiency and net reduction of CO_2 emissions, indicating better economical benefits for the hybrid vehicle with EERS.

Reviewing those investigations above, WHR systems were applied and studied mainly on heavy-duty diesel engines and light-duty vehicle gasoline engines independently. However, little information available has been reported on systematical comparisons and evaluations between the two applications, which is a particularly necessary summary for clarifying the differences. Therefore, this paper provides quantitative comparisons through analyzing EERS applied on a typical heavy-duty diesel engine and a light-duty vehicle gasoline engine, using four attractive working fluids including water, R141b, R123 and R245fa, in order to identify the pros and cons for the two systems and offer general considerations for selections. The thermal efficiency improvement and the reduced CO_2 emission are chosen to be the objective functions to assess the system benefits. The total heat transfer area per net power output (*APP*), the electricity production cost (*EPC*) and the payback period (*PBP*) are examined from the view point of thermo-economics.

Table 1
Specifications for engines used in this investigation.

Parameters	Diesel engine	Gasoline engine
Bore (m)	0.126	0.0825
Stroke (m)	0.130	0.0842
Displacement (cm^3)	6000	1798
Compression ratio	17:1	9.5:1
Injection system	Common rail	Direct injection

Table 2
Main parameters for the diesel engine and the gasoline engine.

Engine load	25%		50%		75%		100%	
	Diesel	Gasoline	Diesel	Gasoline	Diesel	Gasoline	Diesel	Gasoline
Power (kW)	58.8	20	117.7	42.5	176.2	63.7	235.8	84
Efficiency	38.1%	20.8%	41.7%	25.6%	42.2%	28.8%	41.8%	28.1%
T_{exh}[a] (°C)	326	634	420	686	474	758	519	785
m_{exh}[b] (kg/s)	0.127	0.034	0.17	0.059	0.223	0.079	0.275	0.107

[a] Exhaust gases temperature.
[b] Exhaust gases mass flow rate.

2. System descriptions

In this study, a typical heavy-duty diesel engine and a light-duty vehicle gasoline engine are used to provide the hot exhaust waste heat for the EERS. The main parameters for the two engines are presented in Table 1. The usual operating speeds for the diesel and gasoline engines are chosen to be 1500 r/min and 4000 r/min, respectively. The experimental data of exhaust gases are shown in Table 2. The air fuel ratio of gasoline engine is usually controlled to a stoichiometric ratio of 14.8 to maintain a high efficiency of the three-way catalytic converter. Therefore, the composition of the exhaust gases on the basis of mass is assumed to be constant under different engine loads, the results are calculated as: x_{CO2} = 19.84%, x_{H2O} = 8.26%, x_{N2} = 71.49%. However, the air fuel ratio for diesel engine is always variable to optimize combustion, leading to the change of exhaust gas composition under different engine loads, as shown in Table 3. Then the corresponding parameters of exhaust gases, such as the specific heat and the enthalpy, can be obtained with a method for ideal mixture gas under a specific temperature and pressure.

The RC system layout and its corresponding T–s diagram (taking water for example) are shown in Figs. 1 and 2. The system operates in subcritical state, mainly consisting of evaporator, turbine, condenser and pump. The hot exhaust gases from engine rejects the heat to the working fluid, and then the generated high pressure vapor (state 4) flows into the turbine and its enthalpy is converted into power. The process from 4 to 5 s means the isentropic expansion in ideal state. The low-pressure exhaust vapor (state 5) is led to the condenser where it is liquefied by cooling water. The saturated liquid (state 7) available at the condenser outlet is pumped to high pressure (state 1) by pump and then flows into the evaporator, a new cycle begins again.

3. Mathematical models

In the procedure, pinch point temperature difference (PPTD) method is applied. Considering the constraints of the evaporator design and the maximum thermal steady temperature of the working fluid, the PPTD can only occur in the state 2 of working fluid and the outlet of exhaust gas. The initial PPTD is assumed in the state 2, and the value is set to be 30 °C, then the working fluid mass flow rate and the exhaust temperature at the other points would be obtained by the energy balance. The temperature difference in the outlet of exhaust gas would be compared with PPTD and might be assigned with the PPTD value if it is the minimum. It should be mentioned that the exhaust outlet temperature should be kept over 120 °C in order to avoid the dew formation, thus the procedure would regulate the PPTD value to satisfy the minimum exhaust temperature.

Table 3
Composition of exhaust gases for diesel engine.

Engine load (%)	CO_2 (%)	H_2O (%)	O_2 (%)	N_2 (%)
25	9.1	3.5	12.8	74.6
50	12.4	4.8	9	73.8
75	13.9	5.5	7.2	73.4
100	15.2	6	5.8	73

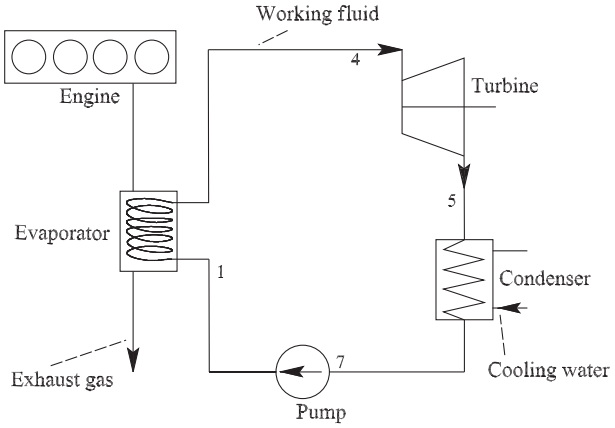

Fig. 1. Schematic diagram of the EERS based on RC.

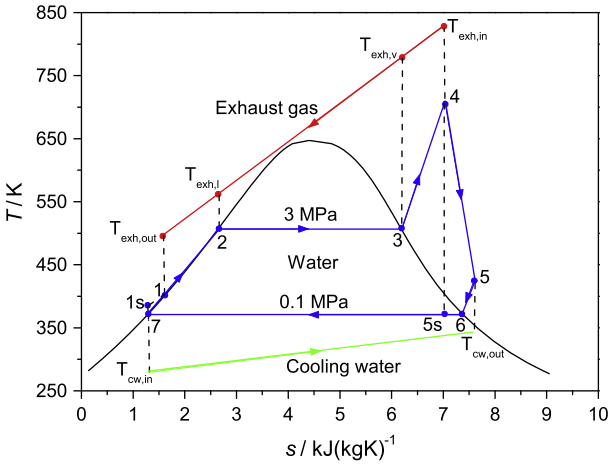

Fig. 2. T–s diagram of RC.

3.1. Thermodynamic model

Several assumptions should be clarified for this study: each component is considered as a steady-state steady-flow system, the kinetic and potential energies as well as the heat and friction losses are neglected. Shell and tube heat exchanger is used as evaporator owing to the high temperature of exhaust gas from engine, with the geometric parameters are listed in Table 4. Plate type heat exchanger is used in the condenser due to its compactness and

Table 4
Geometric dimensions of the for shell and tube evaporator.

Item	Parameter
Number of tube bundles	3
Total number of tubes	5
Tube outside diameter (m)	0.014
Tube inner diameter (m)	0.0116
Shell inner diameter (m)	0.15
Length of tube (m)	0.9
Tube material	Stainless steel
Tube row alignment	Staggered type

high heat transfer coefficient and its information refers to [23]. The isentropic efficiency of turbine and pump is 0.7 and 0.8. The following sections introduce the equations used to perform the analysis.

Evaporator

$$Q_e = m_w(h_4 - h_1) = c_p m_{exh}(T_{exh,in} - T_{exh,out}) \tag{1}$$

Expander

$$W_t = m_w(h_4 - h_5) = m_w(h_4 - h_{5s})\eta_{\exp} \tag{2}$$

Condenser

$$Q_c = m_w(h_5 - h_7) = m_{cw}(h_{cw,out} - h_{cw,in}) \tag{3}$$

Pump

$$W_p = m_w(h_1 - h_7) = m_w(h_{1s} - h_7)/\eta_p \tag{4}$$

The net power output is obtained by

$$W_{net} = W_t - W_p \tag{5}$$

The thermal efficiency improvement of engine-EERS is defined as follows:

$$EI = \frac{W_{net}}{Q_{fuel}} = \frac{W_{net}}{W_{eng}/\eta_{eng}} \tag{6}$$

Here, it should be noted that the improvement is compared not in relative but in absolute value so that the benefit could be shown more directly and obviously.

An analysis of energy conversion was conducted based on the US Electric Power Annual. If the present prototype is used instead of a petroleum-fired power plant, the reduced CO_2 emission M_{CO2} per year can be simply estimated as [24]:

$$M_{CO2} = a_{CO2} t W_{net} \tag{7}$$

where a_{CO2} represents the amount of CO_2 emission if 1 kW h of electrical energy is produced by a petroleum power plant, t is the overall operating time per year, the values are assumed as follows: a_{CO2} = 0.894 kg/(kW h), and t = 8000 h.

3.2. Heat exchangers model

The logarithmic mean temperature difference (*LMTD*) method is used in the heat exchangers model. The heat transfer rate is described as

$$Q = U \cdot A \cdot LMTD \tag{8}$$

In this study, the plate type condenser model refers to the research [23]. Here, only the shell and tube evaporator model is introduced in details.

The overall heat transfer coefficient for shell and tube heat exchanger, U is defined by

$$\frac{1}{U} = \frac{1}{\alpha_i}\frac{d_o}{d_i} + \frac{d_o}{2\lambda}\ln\frac{d_o}{d_i} + \frac{1}{\alpha_o} \tag{9}$$

$$\alpha = \frac{\lambda Nu}{d} \tag{10}$$

Zhukauskas correlation [25] is applied for the exhaust gas in shell side of heat exchanger.

When $1000 < Re < 2 \times 10^5$,

$$Nu_{exh} = 0.35\varepsilon Re_{exh}^{0.6} Pr_{exh}^{0.36}\left(\frac{Pr_{exh}}{Pr_{exh,wall}}\right)^{0.25} \tag{11}$$

When $Re < 1000$,

$$Nu_{exh} = 0.71\varepsilon Re_{exh}^{0.5} Pr_{exh}^{0.36}\left(\frac{Pr_{exh}}{Pr_{exh,wall}}\right)^{0.25} \tag{12}$$

For the single phase working fluid in the tube side, Gnielinski correlation [26] is used to calculate the Nusselt number when $2300 < Re < 10^6$,

$$Nu_w = \frac{(f/8)(Re_w - 1000)Pr_w}{1 + 12.7\sqrt{f/8}(Pr_w^{2/3} - 1)}\left[1 + \left(\frac{d}{l}\right)^{2/3}\right]C_t \tag{13}$$

$$f = (1.82 lg Re_w - 1.64)^{-2} \tag{14}$$

For liquid:

$$C_t = \left(\frac{Pr_w}{Pr_{wall}}\right)^{0.01}, \quad \frac{Pr_w}{Pr_{wall}} = 0.05 - 20 \tag{15}$$

For vapor:

$$C_t = \left(\frac{T_w}{T_{wall}}\right)^{0.45}, \quad \frac{T_w}{T_{wall}} = 0.5 - 1.5 \tag{16}$$

While $Re < 2300$, uniform wall temperature condition is assumed for the laminar flow, the correlation is as follows [25]:

$$Nu_w = 3.66 \tag{17}$$

The boiling heat transfer coefficient for working fluid is calculated by [27]

$$Nu_w = 0.087 Re_w^{0.6} Pr_w^{0.167}\left(\frac{\rho_l}{\rho_v}\right)^{0.2}\left(\frac{\lambda_{wall}}{\lambda_l}\right)^{0.09} \tag{18}$$

3.3. Thermo-economics model

Three economic indicators are put forward and analyzed in this study. The first objective function is the total heat transfer area per net power output (*APP*).

$$APP = A/W_{net} \tag{19}$$

This criterion represents the cost-effectiveness of EERS, as well as the compactness of the system due to the largest contribution of heat exchangers on the total system size, this is particularly essential for the application on internal combustion engines.

Secondly, the electricity production cost (*EPC*), which is the ratio of the total system cost to the net power output, is used to evaluate the system economy.

$$EPC = (CRF \times Cc + Com)/(W_{net} \times t) \tag{20}$$

where *Com* means the operation and management (O&M) cost of the system, which is the 1.65% cost of the *Cc* [28,29].

CRF stands for the capital recovery cost and could be estimated based on the following formula:

$$CRF = \frac{i(1+i)^{LT}}{(1+i)^{LT} - 1} \tag{21}$$

where i is the interest rate and set as 5%, and LT is the system operation lifetime and set as 15 years [29].

Table 5
Coefficients in equations for calculating the investment of system components [23].

Component	K_1	K_2	K_3	B_1	B_2	C_1	C_2	C_3	F_m	F_{bm}
Evaporator	3.853	0.424	0	1.53	1.27	0	0	0	2.8	/
Condenser	3.853	0.424	0	1.53	1.27	0	0	0	2.8	/
Turbine	3.514	0.589	0	/	/	/	/	/	/	3.5
Pump	3.579	0.321	0.003	1.8	1.51	0.168	0.348	0.484	1.8	/

Table 6
Specifications for the simulation conditions in [32].

Parameter	Value
Exhaust gas temperature (°C)	470
Exhaust gases mass flow rate (kg/s)	4.35
Condensation temperature (°C)	35
Turbine isentropic efficiency	0.7
Pump isentropic efficiency	0.8
Pinch point temperature difference (°C)	30
Minimum exhaust outlet temperature (°C)	120

Table 7
Comparison of the present results with the reference data.

	p_e (MPa)	η_c	W_{net} (kW)	m_f (kg/s)	υ_5/υ_4[a]	Source
Benzene	2	0.199	349.3	2.737	107	[33]
	2.009	0.198	347.2	2.717	108	Present
Deviation	0.4%	0.5%	0.6%	0.7%	0.9%	
R11	3.836	0.166	290.3	7.487	32	[33]
	3.836	0.161	281.6	7.95	36	Present
Deviation	0	3%	3%	6%	12.5%	
R134a	3.723	0.085	147.5	8.967	5	[33]
	3.723	0.086	148.2	8.835	5	Present
Deviation	0	1.2%	0.5%	1.5%	0	

[a] Expansion ratio.

Table 8
Properties of the working fluids used in this investigation.

Parameters	R123	R245fa	R141b	Water
Molecular weight (g/mol)	152.9	134	117	18
Normal boiling temperature (°C)	27.8	15.2	32	99.6
Critical pressure (MPa)	3.66	3.65	4.46	22
Critical temperature (°C)	183.7	154	206.85	374
Maximum temperature (°C)	326.85	166.85	226.85	1001.85
ODP/GWP	0.02/77	0/1030	0.12/725	0/<1
Type	Isentropic	Isentropic	Isentropic	Wet

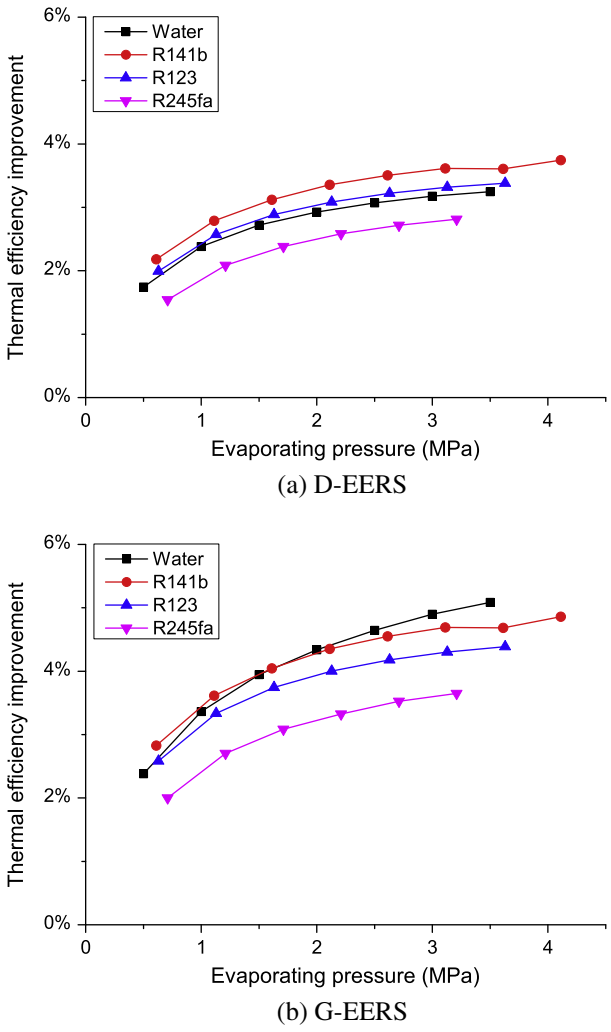

Fig. 3. Thermal efficiency improvement as evaporating pressure under full load.

Cc signifies the capital cost of EERS, comprising the investments for evaporator, turbine, condenser and pump.

$$Cc = (C_{bm,e} + C_{bm,t} + C_{bm,c} + C_{bm,p})CEPCI_{2012}/CEPCI_{1996} \quad (22)$$

where *CEPCI* is the Chemical Engineering Plant Cost Index, which is published in the Chemical Engineering Journal and allows adjusting process plant construction costs from one period to another. Here the component investments are calculated based on the case for 1996.

Each component investment could be predicted by the following correlations [30]. The coefficients K_i, B_i, C_i (i = 1, 2, 3) and F_m are listed in Table 5.

Heat exchangers (evaporator or condenser, taking evaporator as an example):

$$C_{bm,e} = C_e F_{bm} \quad (23)$$

$$\lg C_e = K_{1,e} + K_{2,e} lgA_e + K_{3,e}(lgA_e)^2 \quad (24)$$

$$F_{bm,e} = B_{1,e} + B_{2,e} F_{m,e} F_e \quad (25)$$

$$\lg F_e = C_1 + C_2 \lg(p_e - p_0) + C_3(\lg(p_e - p_0))^2 \quad (26)$$

Turbine:

$$C_{bm,t} = C_t F_{bm,t} \quad (27)$$

$$\lg C_t = K_{1,t} + K_{2,t} lgW_t + K_{3,t}(lgW_t)^2 \quad (28)$$

Pump:

$$C_{bm,p} = C_p F_{bm,p} \quad (29)$$

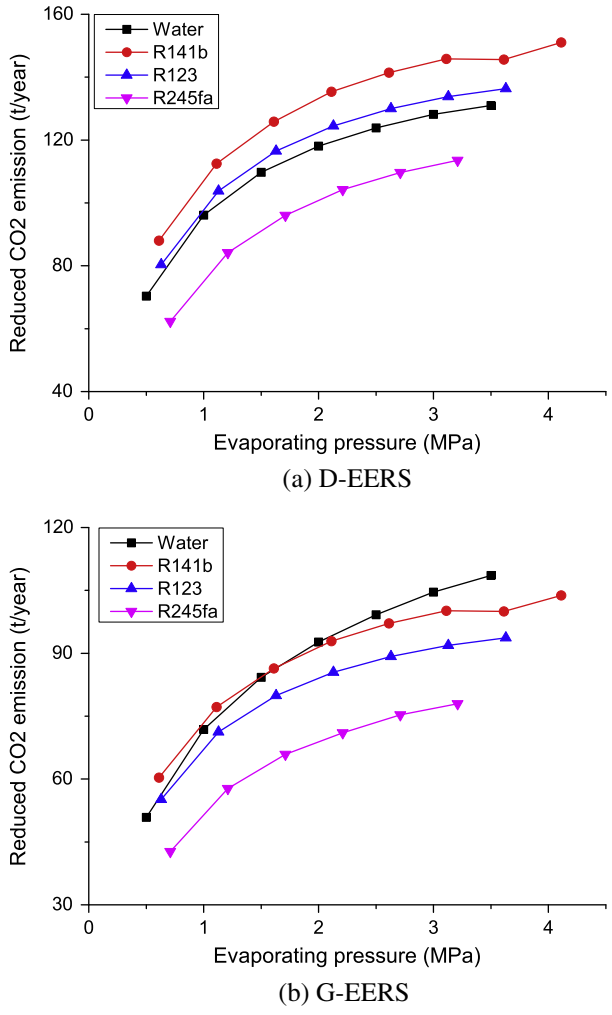

Fig. 4. Reduced CO_2 emission as evaporating pressure under full load.

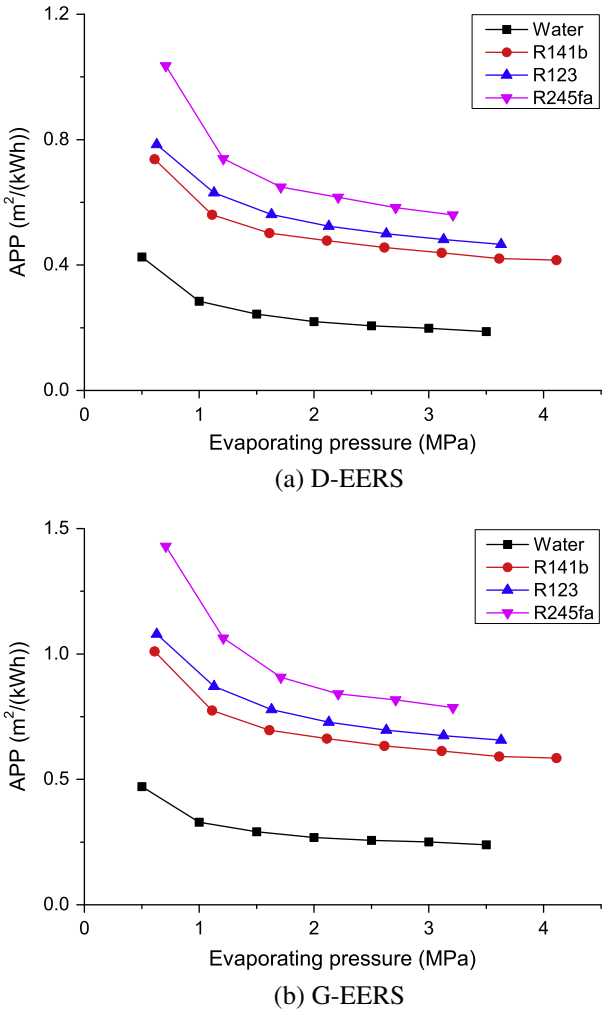

Fig. 5. Total heat exchanger area per power output as evaporating pressure under full load.

$$\lg C_p = K_{1,p} + K_{2,p} IgW_p + K_{3,p}(IgW_p)^2 \tag{30}$$

$$F_{bm,p} = B_{1,p} + B_{2,p} F_{m,p} F_p \tag{31}$$

$$\lg F_p = C_{1,p} + C_{2,p} \lg p_{rp} + C_{3,p}(\lg p_{rp})^2 \tag{32}$$

$$p_{rp} = p_e - p_c \tag{33}$$

The third objective function is the payback period (*PBP*), which represents how soon the investment would be recovered by the income produced by the project, in other words, it means how soon the project would bring about retained profits.

$$PBP = \lg(R/(R - iCc))/lg(1 + i) \tag{34}$$

$$R = M_{pe} t C_{pri} - Com \tag{35}$$

where C_{pri} indicates the average price of diesel or gasoline and set to 8165 ¥/t and 8991 ¥/t for transportation industry in China and it should be transferred into the dollar in US with the average exchange rate of 6.3 in 2012 [31]. It should be mentioned that every project allow a base payback period, otherwise it would be unworthy to be invested. The base value for EERS is considered to be 15 years in China [32].

M_{pe} represents the amount of saved petroleum per year for single system if EERS is used instead of a petroleum-fired power plant [24]:

$$M_{pe} = a_{pe} t W_{net} \tag{36}$$

where a_{pe} is the amount of petroleum consumed to produce 1 kW h of electrical energy, a_{pe} = 0.266 L/(kW h).

4. Validation

To validate the present numerical method, cases of Vaja et al. [33] were chosen for comparison. The simulation conditions in the reference were listed in Table 6. Evaporating pressure varied between condensation pressure and critical pressure. As shown in Table 7, the comparison shows a good agreement between present solutions and the reference results. The deviations of different parameters mainly derive from the different measurements when the exhaust outlet temperature decreased lower than 120 °C, the procedure in [33] decreased the working fluid mass flow rate, meaning that there were no the pinch point limitations in the heat exchange process. However, this accuracy is believed to be sufficient for most engineering applications.

5. Results and discussion

Based on the experiment data of exhaust gases from diesel and gasoline engines in Section 2 and the mathematic methods in Section 3, four attractive working fluids including Water, R123, R141b and R245fa are examined to explore further their maximum

potential of system benefits and thermo-economics. Therefore, water would operate under 0.1 MPa to perform as well as possible and avoid leakage at condenser at the same time, while the organic fluids with low boiling temperature would work at 35 °C of condensing temperature to guarantee the pinch point temperature difference of 5 °C between the fluid and cooling water in the condenser. Evaporating pressure varies between condensing pressure and critical pressure. The working fluid temperature in the outlet of evaporator is kept no less than the saturated temperature to guarantee the dry expansion in the turbine, meaning necessary superheating would be required when the quality in the outlet of turbine is lower than 1, especially for the wet fluid water. The physical properties of the four working fluids are listed in Table 8.

In the following analysis, the influences of evaporating pressure on the system performances would be discussed under full engine load and the optimal pressure would be found out. Then the effect of engine type and load would be examined under optimized condition to compare the best results for each load and working fluid. Here, the heavy-duty diesel engine and light-duty vehicle gasoline engine are represented with D and G for simplifications, and the corresponding system is D-EERS and G-EERS, respectively. The thermal efficiency improvement and the reduced CO_2 emission are chosen to be the objective functions to assess the system benefits. The total heat transfer area per net power output (*APP*), the electricity production cost (*EPC*) and the payback period (*PBP*) are examined from the view point of thermo-economics.

5.1. Effect of evaporating pressure

Figs. 3 and 4 presents the influences of evaporating pressure on the system gains, including the thermal efficiency improvement and the reduced CO_2 emission, taking the full load as an example. It could be found that increasing pressure would achieve better gains due to the rise of power output. For a certain working fluid under the specific engine load, when the evaporating pressure is boosted, with the condensing pressure constant, the pressure ratio during the expansion in turbine would be enlarged, resulting into the increase of enthalpy drop in the expander, meanwhile, the working fluid mass flow rate would be decreased due to the reduction of heat transferred in the evaporator with the limitation of PPTD. In the beginning of pressure increase, the increase of enthalpy drop overweighs largely the decrease of mass flow rate, the power output as well as the thermal efficiency improvement boosts quickly, as the pressure rises up further, the gradient gap between the two factors of power output would be reduced, thus the curves in the figures would level off for the high pressure.

For the D-EERS, R141b shows the best performances, followed by R123 and water, while R245fa offers the worst profits. Water exhibits distinctive feature in the G-EERS, just like "chasing and surpassing" to become the best candidate at higher pressure. This could be explained by the fact that exhaust gas of gasoline engine presents high temperature property which is more applicable for fluids like water owning considerably high boiling temperature.

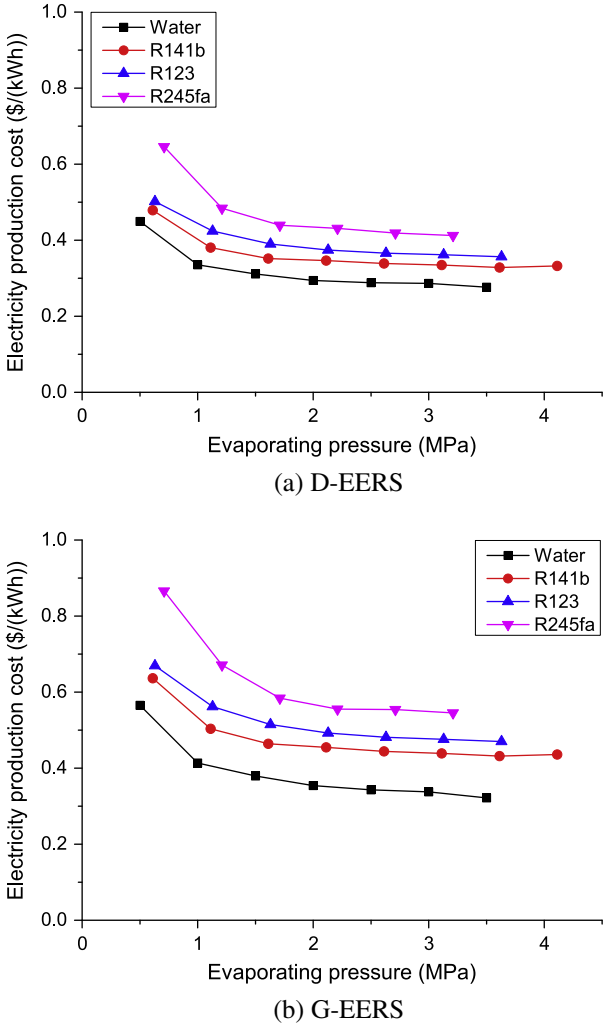

Fig. 6. Electricity production cost as evaporating pressure under full load.

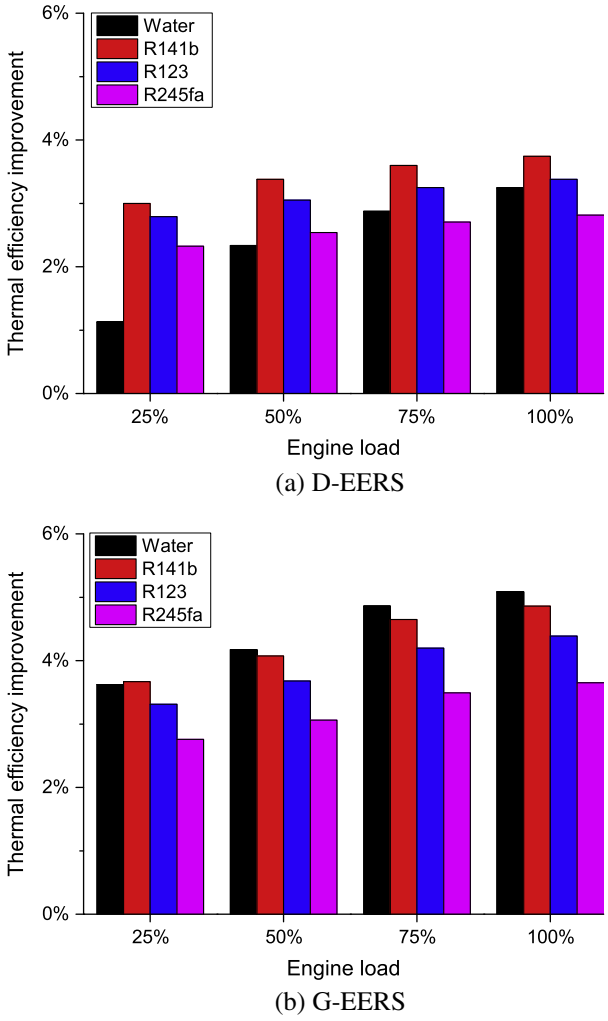

Fig. 7. Thermal efficiency improvement as engine load.

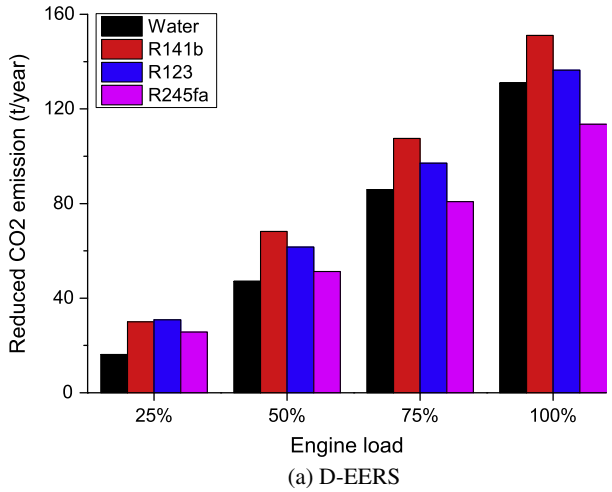

Fig. 8. Reduced CO_2 emission as engine load.

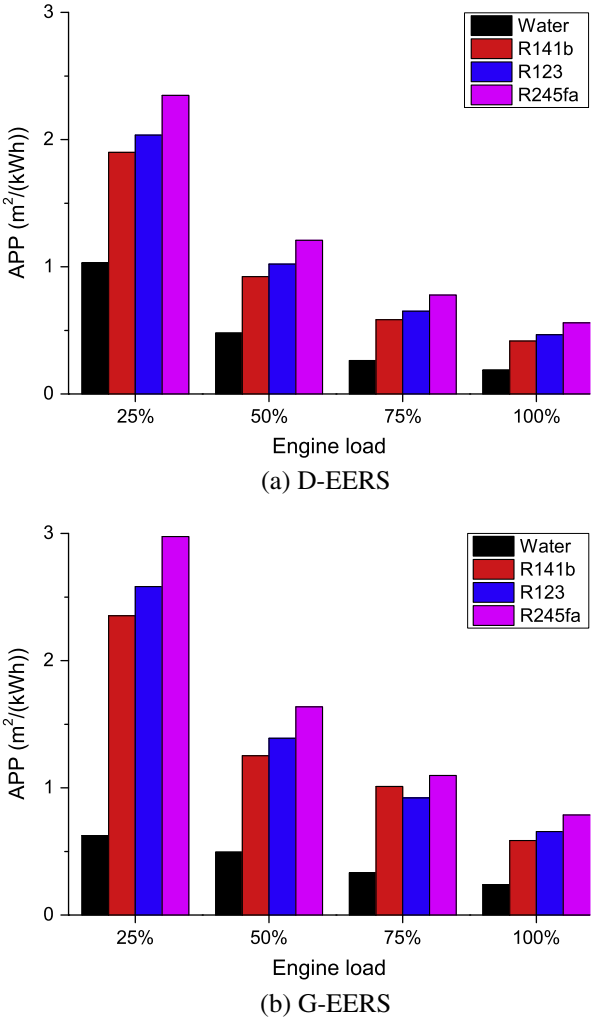

Fig. 9. Thermal efficiency improvement as engine load.

Comparatively, diesel engine discharges exhaust energy with lower temperature, which is more appropriate to be recovered by organic fluids with low boiling temperature.

As shown in Fig. 4, the capability of EERS to reduce CO_2 emission shows the similar tendency with its contributions on the thermal efficiency improvement. The reason for this could be inferred by the Eqs. (6) and (7), in which the reduced CO_2 emission is directly determined by the increasing power output, while the latter presents proportional to the thermal efficiency improvement. Actually, the reduction of greenhouse gases benefits from the saving of fuel consumption due to the introducing of EERS on ICE.

The system cost-effectiveness as evaporating pressure could be observed in Fig. 5. Similarly, higher pressure would yield lower *APP*, saving the cost of heat exchangers to produce the same power output. As the pressure is enhanced, the area of heat exchanger would be reduced due to the improvement of heat transfer, as well as the power output would be increased. Therefore, their ratio *APP* would decrease rapidly first and then go to smooth.

Among the fluids, water is the most economical one with lowest *APP* value both for the two EERS. This is also attributed to its high boiling temperature which allows higher pinch point temperature difference between the fluid and cooling water in the condenser, directly requiring less condenser area. For the other fluids, their low boiling temperature limits largely the temperature difference in the condenser, leading to much higher condenser size.

Another thermo-economic performance is represented by *EPC*, which is shown in Fig. 6. Its variations as evaporating pressure for different working fluids are similar to the results of *APP*. This is because of their close relevance, larger *APP* means a higher necessity of heat exchanger areas, which accounts for the most investments among the system capital cost [34], subsequently, higher expense would be taken to produce the same power output.

5.2. The effect of engine type and load

The analysis above reveals that higher pressure benefit for system performances. Therefore, the results at optimal pressure of working fluids are examined here, in order to explore the maximum potential of EERS for the four fluids. Figs. 7 and 8 gives the best performances for each working fluid under different engine loads. It could be witnessed that G-EERS presents slightly superior to D-EERS in the improvement of thermal efficiency. This is most likely from the fact that gasoline engine performs with much lower thermal efficiency than diesel engine, which could be found in Table 2, thus the former exists larger potential to be improved in efficiency. Even so, the difference between the two results is considered to be quite small, with less than 1.5% point. The peak improvement in efficiency is achieved by R141b for D-EERS and water for gasoline one both at full load, which is 3.7% and 5.1% point in absolute, respectively. Yet the D-EERS reduce much more greenhouse gas emission due to more power output. The maximum amount of reduced CO_2 emission is realized by the former as high as 150 t/year, compared with 110 t/year for the latter.

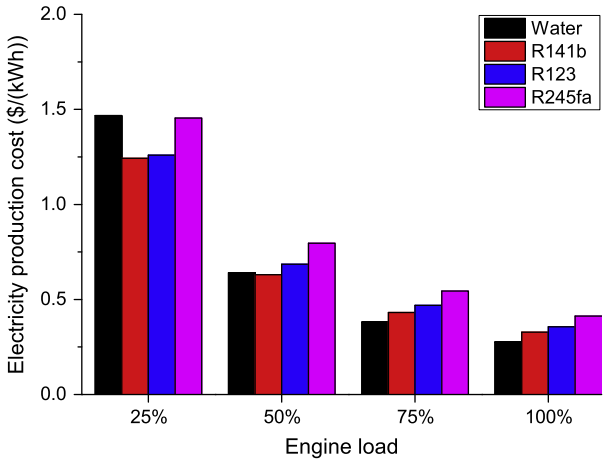

(a) D-EERS

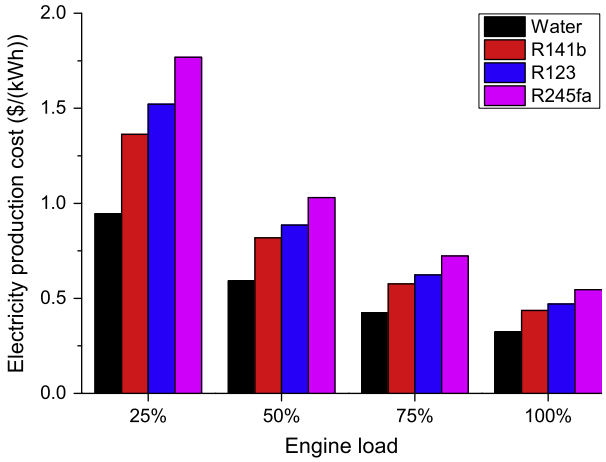

(b) G-EERS

Fig. 10. Electricity production cost as engine load.

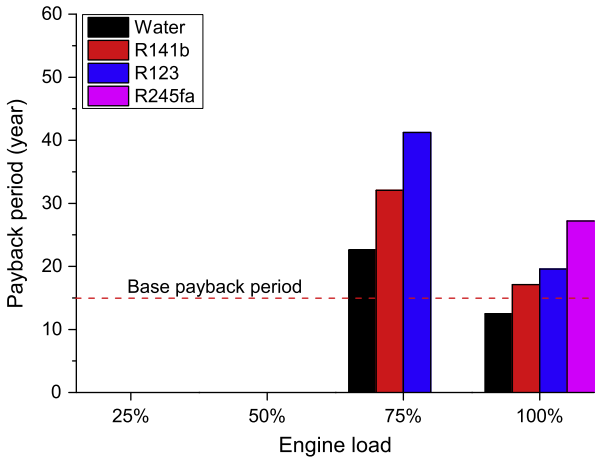

(a) D-EERS

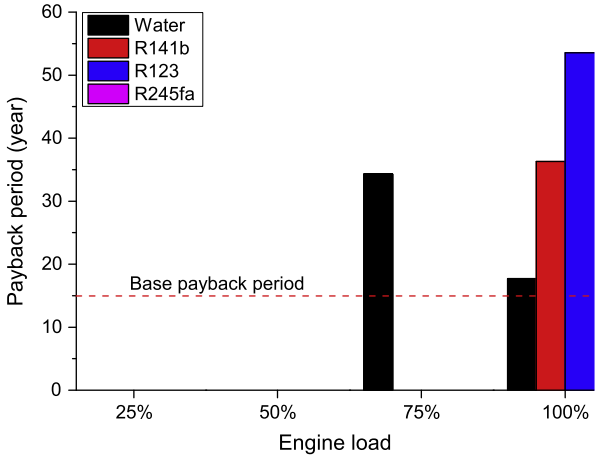

(b) G-EERS

Fig. 11. Payback period as engine load.

Increasing the engine load would bring about more contributions both in the two aspects. Higher engine load means more exhaust heat could be provided, and the heat transfer would also become better as the exhaust gases temperature rises up. These would contribute more power output, thus give rise to better thermal efficiency improvement and reduce more CO_2 emission.

Water shows different performances under the two systems. In the D-EERS, water works inferior to most other fluids owing to the relative low exhaust temperature of diesel engine, making inadequate heat transfer between water and exhaust gases. While for G-EERS, hot exhaust temperature guarantee the enough heat amount absorbed and more power output produced by water.

The *APP* and *EPC* values under different engine types and loads could be depicted in Figs. 9 and 10. It could be seen clearly that D-EERS requires smaller heat exchangers and lower cost compared with the gasoline one for the same electricity production, indicating that it is more applicable for EERS on the diesel engine. And higher engine load would be attractive for cost-effectiveness and thermo-economics. This is also attributed to the more exhaust heat and the better heat transfer in the evaporator, as the engine load boosts. Among the fluids, water serves the best candidate with the lowest *APP* and *EPC* values, followed by R141b and R123, while R245fa expends the most to operate.

The results in Fig. 10 also reveal that engine load influence strongly the performance of water in the D-EERS, which could be embodied by its decreasing *EPC* difference compared with those of other fluids, especially when the engine load increases up to 75%, the difference reduces down to negative, meaning it starts to become more economical than others. This could be explained by the fact that increasing engine load directly boosts the exhaust heat amount, particularly augments the exhaust temperature, thus water with high boiling temperature and evaporation latent would better follow the exhaust temperature profile, which would benefit greatly for the heat transfer process. More exhaust heat is absorbed by water and higher power output is produced maintaining the relative low heat transfer areas. For the gasoline engine at speed as high as 4000 r/min, as shown in Table 2, the exhaust temperature is high enough even under the low load, to satisfy the excellent heat transfer between water and the hot heat source, so water in the G-EERS could be superior to other fluids under all the loads.

Fig. 11 shows the payback period of EERS under different engine loads. Here it reflects the risk of investment on the EERS and gives the assessment for the economic possibility of technology application. Similarly, the *PBP* value will get smaller at higher engine load. As mentioned above, enhancing engine load would achieve higher *EI* and expend lower *EPC*, means that the gap between the profits and costs, which here could be characterized with PBP, would be reduced.

The blank spaces in the figures demonstrate that the incomes produced by the EERS could not afford the sum of capital cost and O&M cost, even could not offset the cost for O&M, i.e. no net return all the time. For example, when the D-EERS operates only

under 25% and 50% load, the investments would not be recovered, the same case for G-EERS implies worse since only water could give a foreseeable time to achieve the payback.

However, situation might be more pessimistic if the base payback period is considered. The red dotted line is the base payback period which is the tolerant time for deficit of the invested project in the industry, it is considered to be 15 years for the power industry in China [30]. Among the fluids, R245fa is the most uneconomical that could not payback the cost for all the cases. R141b and R123 exhibit relatively better and have the potential to be applied if some optimizations for the system are developed, water presents the exclusive advantage to realize profits.

It could be found that only the D-EERS using water as working fluid under the full load meet the economic demand. In general, the G-EERS performs worse in thermo-economics. Besides, the gasoline engines operates in variable loads and covers wide speeds, meanwhile proposes rigorous space limitations for the downsizing vehicle, which would put forward more tough difficulties and challenges on the application of EERS. On the whole, the EERS based on RC serve better on the heavy-duty diesel engine, while it seems not to be applicable for the light-duty vehicle gasoline engine at least in the current, unless the state-of-the art technologies, such as EERS optimizations in efficiency, downsizing and response controls, are developed in the future.

6. Conclusions

In this study, quantitative comparisons are carried out for exhaust energy recovery system (EERS) applied on a typical heavy-duty diesel engine (D) and a light-duty vehicle gasoline engine (G), using water, R141b, R123 and R245fa as the working fluids of Rankine cycle (RC). The influences of evaporating pressure, engine type and load on the system performances are analyzed and discussed, with multi-objectives as criterions such as the thermal efficiency improvement, the reduced CO_2 emission, the total heat transfer area per net power output (*APP*), the electricity production cost (*EPC*) and the payback period (*PBP*). Several conclusions are drawn as follows:

(1) Increasing pressure and engine load would benefit for better performances, with higher improvements in efficiency, more reduced CO_2 emission, lower *APP* and *EPC* level. Besides, engine load influence strongly the performance of water in the diesel EERS. Low engine load would be undesired to payback, let alone make profits.
(2) For the D-EERS, R141b shows the best performances with 3.7% increase in efficiency and 150 t/year reduction in CO_2 emission, followed by R123 and water, while R245fa offers the worst profits. In the G-EERS Water exhibits the largest contributions, with 5.1% efficiency improvement and CO_2 emission reductions as high as 110 t/year. In terms of thermo-economics, water serves the best candidate with the lowest *APP* and *EPC* values, as well as exclusive advantage to realize profits, followed by R141b and R123, while R245fa expends the most to operate and hard to recover the investments.
(3) The D-EERS presents superior to the G-EERS with better economical applicability as well as much more CO_2 emission reductions, in spite of slightly lower thermal efficiency improvement. And only the D-EERS using water as working fluid under the full load meets the economic demand.

In general, the EERS based on RC serves not applicable for the light-duty vehicle gasoline engine at least in the current and might be feasible as the state-of-the art technologies, such as EERS optimizations in efficiency, downsizing and response controls, are developed in the future. This study could provide a preliminary attempt to explore the pros and cons of the applications, although the comparisons are conducted on the two particular engines. Further researches will be carried out to expand this comparison in a broader spectrum and come to universal recommendations in future works.

Acknowledgements

Financial supports from the National Basic Research Program of China (973 Program) through the project of 2011CB707201 and the National Natural Science Found of China (NSFC) through the project of 50876074 are gratefully acknowledged.

References

[1] Wang TY, Zhang YJ, Peng ZJ, et al. A review of researches on thermal exhaust heat recovery with Rankine cycle. Renew Sustain Energy Rev 2011;15:2862–71. http://dx.doi.org/10.1016/j.rser.2011.03.015.
[2] Patel PS, Doyle EF. Compounding the truck diesel engine with an organic Rankine cycle system. SAE paper no. 760343; 1976.
[3] Doyle E, DiNanno L, Kramer S. Installation of a diesel-organic Rankine compound engine in a class 8 truck for a single-vehicle test. SAE paper no. 790646; 1979.
[4] DiBella FA, DiNanno LR, Kaplow MD. Laboratory and on-highway testing of diesel organic Rankine compound long-haul vehicle engine. SAE paper no. 830122; 1983.
[5] Teng H, Regner G, Cowland C. Waste heat recovery of heavy-duty diesel engines by organic Rankine cycle Part I: hybrid energy system of diesel and Rankine engines. SAE paper no. 2007–01-0537; 2007.
[6] Teng H, Regner G. Improving fuel economy for HD diesel engines with WHR Rankine cycle driven by EGR cooler heat rejection. SAE paper no. 2009–01-2913; 2009.
[7] Teng H, Klaver J, Park T, et al. A Rankine cycle system for recovering waste heat from HD diesel engines-WHR system development. SAE paper no. 2011–01-0311; 2011.
[8] Katsanos CO, Hountalas DT, Pariotis EG. Thermodynamic analysis of a Rankine cycle applied on a diesel truck engine using steam and organic medium. Energy Convers Manage 2012;60:68–76. http://dx.doi.org/10.1016/j.enconman.2011.12.026.
[9] Hountalas DT, Mavropoulos GC, Katsanos C. Improvement of bottoming cycle efficiency and heat rejection for HD truck applications by utilization of EGR and CAC heat. Energy Convers Manage 2012;53:19–32. http://dx.doi.org/10.1016/j.enconman.2011.08.002.
[10] Macián V, Serrano JR, Dolz V, et al. Methodology to design a bottoming Rankine cycle, as a waste energy recovering system in vehicles. Study in a HDD engine. Appl Energy 2013;104:758–71. <http://dx.doi.org/10.1016/j.apenergy.2012.11.075>.
[11] Shu GQ, Liu LN, Tian H, et al. Analysis of regenerative dual-loop organic Rankine cycles (DORCs) used in engine waste heat recovery. Energy Convers Manage 2013;76:234–43. <http://dx.doi.org/10.1016/j.enconman.2013.07.036>.
[12] Shu GQ, Liu LN, Tian H, et al. Parametric and working fluid analysis of a dual-loop organic Rankine cycle (DORC) used in engine waste heat recovery. Appl Energy 2014;113:1188–98. <http://dx.doi.org/10.1016/j.apenergy.2013.08.027>.
[13] Shu GQ, Liu LN, Tian H, et al. Performance comparison and working fluid analysis of subcritical and transcritical dual-loop organic Rankine cycle (DORC) used in engine waste heat recovery. Energy Convers Manage 2013;74:35–43. <http://dx.doi.org/10.1016/j.enconman.2013.04.037>.
[14] Oomori H, Ogino S. Waste heat recovery of passenger car using a combination of Rankine bottoming cycle and evaporative engine cooling system. SAE paper no. 930880; 1993.
[15] Chammas RE, Clodic D. Combined cycle for hybrid vehicles. SAE paper no. 2005–01-1171; 2005.
[16] Ringler J, Seifert M, Guyotot V, et al. Rankine cycle for waste heat recovery of IC engines. SAE paper no. 2009–01-0174; 2009.
[17] Horst TA, Rottengruber HS, Seifert M, et al. Dynamic heat exchanger model for performance prediction and control system design of automotive waste heat recovery systems. Appl Energy 2013;105:293–303. <http://dx.doi.org/10.1016/j.apenergy.2012.12.060>.
[18] Arias DA, Shedd TA, Jester RK. Theoretical analysis of waste heat recovery from an internal combustion engine in a hybrid vehicle. SAE paper no. 2006–01-1605; 2006.
[19] Endo T, Kawajiri S, Kojima Y, et al. Study on maximizing exergy in automotive engines. SAE paper no. 2007–01-0257; 2007.
[20] Wang TY, Zhang YJ, Zhang J, et al. Analysis of recoverable exhaust energy from a light-duty gasoline engine. Appl Therm Eng 2013;53:414–9. http://dx.doi.org/10.1016/j.applthermaleng.2012.03.025.
[21] Wang EH, Zhang HG, Zhao Y, et al. Performance analysis of a novel system combining a dual loop organic Rankine cycle (ORC) with a gasoline engine. Energy 2012;43:385–95. http://dx.doi.org/10.1016/j.energy.2012.04.006.

[22] Peng ZJ, Wang TY, He YL, et al. Analysis of environmental and economic benefits of integrated exhaust energy recovery (EER) for vehicles. Appl Energy 2013;105:238–43. <http://dx.doi.org/10.1016/j.apenergy.2013.01.004>.
[23] Tian H, Shu GQ, Wei HQ, et al. Fluids and parameters optimization for the organic Rankine cycles (ORCs) used in exhaust heat recovery of internal combustion engine (ICE). Energy 2012;47:125–36. <http://dx.doi.org/10.1016/j.energy.2012.09.021>.
[24] Yamaguchi H, Zhang XR, Fujima K, et al. Solar energy powered Rankine cycle using supercritical CO_2. Appl Therm Eng 2006;26:2345–54. http://dx.doi.org/10.1016/j.applthermaleng.2006.02.029.
[25] Yang SM, Tao WQ. Heat transfer. 4th ed. Beijing: Higher Education; 2006.
[26] Gnielinski V. New equations for heat mass transfer in turbulent pipe and channel flows. Int Chem Eng 1976;16:359–68.
[27] Klimenko VV. A generalized correlation for two-phase forced flow heat transfer. Int J Heat Mass Trans 1988;31:541–52.
[28] Cayer E, Galanis N, Nesreddine H. Parametric study and optimization of a trans-critical power cycle using low temperature source. Appl Energy 2010;87:1349–57. http://dx.doi.org/10.1016/j.apenergy.2009.08.031.
[29] Schuster A, Karellas S, Kakaras E, et al. Energetic and economic investigation of organic Rankine cycle applications. Appl Therm Eng 2009;29:1809–17. http://dx.doi.org/10.1016/j.applthermaleng.2008.08.016.
[30] Turton R, Bailie RC, et alWhiting WB. Analysis, synthesis and design of chemical processes. 1st ed. New Jersey: Prentice Hall PTR; 1998.
[31] National development and reform commission (NDRC) of People's Republic of China, <http://www.sdpc.gov.cn/zcfb/zcfbtz/2012tz/default.htm, 2012-11-15>.
[32] National development and reform commission (NDRC) and Ministry of construction (MOC) of People's Republic of China, Methods and parameters for economic evaluation of construction project, 3rd ed., China Planning, Beijing, 2006.
[33] Vaja I, Gambarotta A. Internal combustion engine (ICE) bottoming with organic Rankine cycles (ORCs). Energy 2010;35:1084–93. http://dx.doi.org/10.1016/j.energy.2009.06.001.
[34] Papadopoulos AI, Stijepovic M, Linke P. On the systematic design and selection of optimal working fluids for organic Rankine cycles. Appl Therm Eng 2010;30:760–9. http://dx.doi.org/10.1016/j.applthermaleng.2009.12.006.